Aspects of Structure and Bonding in Copper−Amino Acid Complexes Revealed by Single-Crystal EPR/ENDOR Spectroscopy and Density Functional Calculations

Michael J. Colaneri,[†,*] Jacqueline Vitali,[‡,*] and Jack Peisach[§]

Department of Chemistry and Physics, State University of New York at Old Westbury, Old Westbury, New York 11568, Department of Physics, Cleveland State University, Euclid Avenue and East 24th Street, Cleveland, Ohio, 44115 and Department of Physiology and Biophysics, Albert Einstein College of Medicine, 1300 Morris Park Avenue, Bronx, New York 10461

Received: December 19, 2008; Revised Manuscript Received: March 6, 2009

This work deduces from a series of well-defined copper-doped amino acid crystals, relationships between structural features of the copper complexes, and ligand-bound proton hyperfine parameters. These were established by combining results from electron paramagnetic resonance (EPR)/electron−nuclear double resonance (ENDOR) studies, crystallography, and were further assessed by quantum mechanical (QM) calculations. A detailed evaluation of previous studies on Cu^{2+} doped into α-glycine, triglycine sulfate, α-glycylglycine, and L-alanine crystals reveal correlations between geometric features of the copper sites and proton hyperfine couplings from amino-bound and carbon-bound hydrogens. Experimental variations in proton isotropic hyperfine coupling values (a_{iso}) could be fit to cosine-square dependences on dihedral angles, namely, for C_α-bound hydrogens, $a_{iso} = -1.09 + 8.21 \cos^2 \theta$ MHz, and for amino hydrogens, $a_{iso} = -6.16 + 4.15 \cos^2 \varphi$ MHz. For the C_α hydrogens, this dependency suggests a hyperconjugative-like mechanism for transfer of spin density into the hydrogen 1s orbital. In the course of this work, it was also necessary to reanalyze the ENDOR measurements from Cu^{2+}-doped α-glycine because the initial study determined the ^{14}N coupling parameters without holding its nuclear quadrupole tensor traceless. This new treatment of the data was needed to correctly align the ^{14}N hyperfine tensor principal directions in the molecular complex. To provide a theoretical basis for the coupling variations, QM calculations performed at the DFT level were used to compute the proton hyperfine tensors in the four crystal complexes as well as in a geometry-optimized $Cu^{2+}(glycine)_2$ model. These theoretical calculations confirmed systematic changes in couplings with dihedral angles but greatly overestimated the experimental geometric sensitivity to the amino hydrogen isotropic coupling.

Introduction

Electron paramagnetic resonance (EPR) spectroscopy has a long history of the study of copper-doped crystalline systems.[1] The primary aim of these were to obtain accurate and unambiguous g and copper hyperfine and quadrupole tensors to both define the coordination of the doped metal ion and to understand how the observed spectral characteristics relate to electronic structure. Results from single-crystal experiments where doped copper replaced other transition ions in crystalline amino acid models[2] have shown that the site can be identified by alignment of the g and copper hyperfine tensor axes with the ligand bond directions in the host. Such tensor alignments were useful in postulating metal coordination in subsequent studies on molecular crystals, where the copper dopes at specific interstitial sites.[3] The further application of electron−nuclear double resonance (ENDOR) spectroscopy in measuring ligand ^{14}N and nearby ^{1}H hyperfine couplings became very instrumental in supporting the proposed characteristics of copper−molecular complexes.[4−10]

Recent advances in pulsed-EPR (electron spin echo envelope modulation − ESEEM, pulsed-ENDOR, and hyperfine sublevel correlation − HYSCORE) and high-field EPR methods have allowed for the determination of the g and hyperfine tensors in nonoriented copper samples to a precision approaching that was found in single-crystal studies.[11] Although still not as unambiguous as the crystal work, these orientation-averaged studies nevertheless provide information on many important biological systems that cannot be investigated in any other way. However, because of the lack of a priori structural information, the usefulness of these methods in understanding the biological role of copper relies heavily on interpreting weak hyperfine coupling interactions from remote nuclei.[11,12]

The present study aims to proceed further in the analysis of both the amino-bound (H_a) and C_α-bound (H_C) hydrogen ^{1}H hyperfine interactions in copper−amino acid complexes by determining possible correlations between the coupling values and coordination geometry. To do this, an analysis was made of results from four previously published examinations of copper-doped single-crystal amino acids that had been the subject of combined EPR and ENDOR investigations. These were copper-doped α-glycine,[4] triglycine sulfate,[5,6] L-alanine,[7,8] and α-glycylglycine.[9] Figure 1 displays[13,14] the proposed copper sites in the host crystal structures of α-glycine,[15] triglycine sulfate,[16] L-alanine,[17] and α-glycylglycine[18] determined by neutron diffraction experiments. The EPR/ENDOR analyses of these systems were mostly concerned with identifying the copper binding sites, and there has not been any concerted discussion of possible dependences of the ligand couplings on geometric aspects of the copper−amino acid complexes. As mentioned

* To whom correspondence should be addressed. E-mail: colanerim@oldwestbury.edu. Tel: (516) 876-2756. Fax: (516) 876-2749 (M.J.C.), E-mail: j.vitali@csuohio.edu. Tel: (216) 687-2431. Fax: (216) 803-2027 (J.V.).
† SUNY at Old Westbury.
‡ Cleveland State University.
§ Albert Einstein College of Medicine.

10.1021/jp811249s CCC: $40.75
Published on Web 04/20/2009

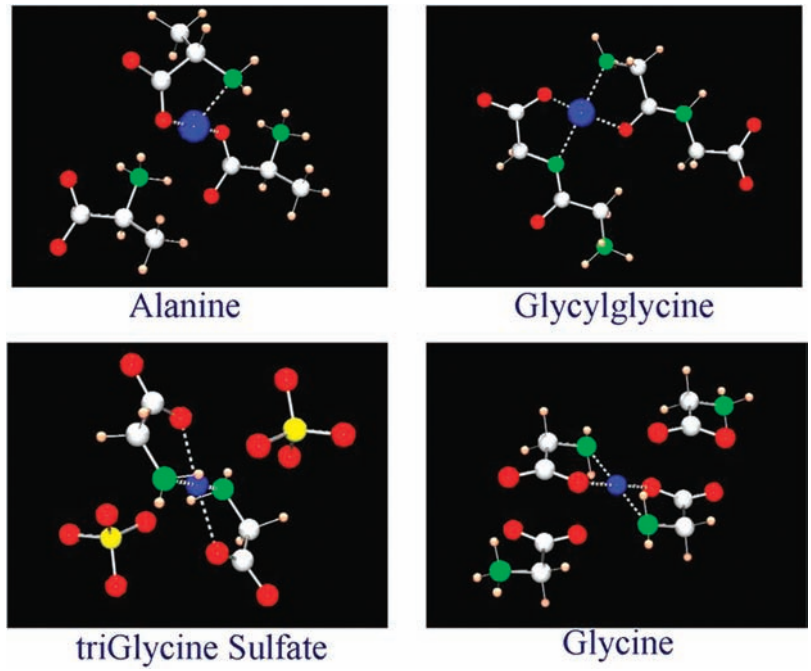

Figure 1. View of the molecular structures of four copper−amino acid complexes; copper-doped L-alanine, α-glycine, glycylglycine, and triglycine sulfate. Atomic coordinates were taken from diffraction studies of the host crystals. The structure views were produced using Ortep-3[13] and rendered by POV-Ray.[14]

above, knowledge on how molecular geometry influences remote magnetic coupling interactions has useful predictive value in the study of biological systems and gives important insight into the electronic structure of copper coordination.

In each case shown in Figure 1, the EPR measured g and Cu^{2+} hyperfine tensors were shown to be consistent with a copper $d_{x^2-y^2}$ ground state, with the equatorial *xy* plane approximately defined by the directly coordinated ligand atoms. It was demonstrated by ENDOR that the coordinated glycine amino nitrogen deprotonates when copper binds, causing the copper complex in glycine to become charge neutral.[4] Similar evidence showing that ligating amino groups may deprotonate by copper binding to give neutral charged complexes come from early EPR "truth tables" of Peisach and Blumberg.[19] The postulated glycine, triglycine, and glycylglycine sites each have trans 2N2O ligation, whereas in alanine a three coordinate N2O complex was proposed.[8] Here, a distant second amino group is located 2.5 Å from copper on the opposite side of the directly coordinated nitrogen. ENDOR results[8] indicate that this distant amino group does not deprotonate, and that leaves the copper complex in alanine with a net positive charge. The copper−alanine system is also different than the others because ^{1}H ENDOR measurements of the amino hydrogens indicate a flattening of the amino group from its original tetrahedral geometry.[8] Additionally, the postulated metal site is one where copper binds the nitrogen at a 90° angle to the N−C_α bond, which is unlike the other systems that have angles closer to tetrahedral. In the copper−glycine complex, carboxylate oxygens from two other zwitterionic glycine molecules are positioned on either side, approximately axial to the equatorial plane. In copper−triglycine sulfate, oxygens from two charged sulfate ions are bound axially, leaving the complex with a net −2 charge. In all four systems, ligand ^{14}N hyperfine and quadrupole couplings, as well as amino-bound and carbon-bound ^{1}H hyperfine tensors, were determined by ENDOR. The relative signs of the C_α-bound and amino proton couplings in triglycine sulfate were established by TRIPLE-ENDOR experiments.[6] In addition, amino-bound ^{2}D hyperfine and quadrupole tensors were obtained in deuterated crystals.[6] In the copper-doped glycine ENDOR study,[4] the ^{14}N coupling parameters were computationally refined without the theoretical constraint that the quadrupole tensor remains traceless.[20] Therefore, published ^{14}N ENDOR frequency data for this system was re-refined to conform to treatments of data in the three other crystal complexes.

With the exceptions of a flattening of the alanine amino group, and reorientations of amino hydrogens about the C_α-N bond in triglycine sulfate (and also presumably in glycine), the molecules coordinating to the doped copper ion in the crystal complexes are assumed to maintain the same structure as found in the host crystals. Support for this comes from (1) the measured g, hyperfine, and quadrupole tensor directions, which have very good correlation with ligand bonds and directions in the native structures, (2) the copper positioned at the inversion center in the α-glycine crystal gives rise to two equivalent pairs of ENDOR coupling tensors, one from each symmetrically equivalent glycine, and (3) the close similarity in the ENDOR measured coupling tensors from the two structurally similar coordinating molecules in triglycine sulfate (molecule II and molecule III). Therefore, any adjustments in the molecular positions or geometries when accommodating the copper are not anticipated to be large enough to significantly alter the trends described below.

A careful analysis of the experimental ^{1}H hyperfine couplings in these systems revealed geometrical correlations with certain dihedral angles in the complexes. To provide a theoretical basis and comparison with the observed dependencies, QM calculations using Kohn−Sham DFT[21,22] were carried out on the crystal complexes in Figure 1 and on a geometry-optimized model of a $Cu^{2+}(glycine)_2$ complex. The QM calculations generated singly occupied molecular orbitals that were consistent with those found in previous QM/DFT treatments of copper−nitrogen and copper−histidine systems.[24,25] In the present model, the dihedral angle between the Cu−N−C_α and N−C_α−H_C planes and the rotation angle of the amino group hydrogens about the C_α−N bond were varied to determine their influence on proton coupling interactions. The previous DFT computations report disparities

TABLE 1: g and ^{14}N Hyperfine A^N and Quadrupole Q^N Coupling Tensors for Copper-Doped α-Glycine[a]

		Direction Cosines		
	Principal Values	*a*	*b*	*c′*
g	2.2644	0.652	0.658	0.378
	2.0715	−0.723	0.387	0.573
	2.0434	0.230	−0.646	0.727
		Direction Cosines		
	Principal Values (MHz)	*a*	*b*	*c′*
$\mathbf{A}^N$	32.44	−0.207	0.751	−0.627
	20.85	0.441	0.644	0.625
	20.62	0.873	−0.147	−0.465
$\mathbf{Q}^N$	1.09	0.980	−0.057	−0.191
	0.16	0.178	0.684	0.707
	−1.25	−0.090	0.727	−0.681

[a] . Tensor principal directions (direction cosines) refer to the crystallographic *abc′* right-handed system, with $c' = a \times b$.

between observed ^{14}N and ^{1}H hyperfine coupling values that were attributed to an overestimation of spin transfer and spin contamination.[22−25] However, these studies also conclude that such deviations are generally systematic for a given atomic basis set, functional and model system, making the prediction of trends in variations of hyperfine couplings in related compounds much more reliable. The results described below may spur further work in improving such theoretical calculations.

Experimental Methods

The previous EPR/ENDOR study of copper-doped glycine crystals possibly used a left-handed coordinate system.[26] This was experimentally confirmed by EPR (Varian E109) X-band spectral measurements at 77 K on copper-doped α-glycine single crystals. The doped crystals were grown using published methods[4] and the beta angle was identified by microscopic examination of the crystal morphology. Spectra were recorded along the crystalline *a*, *b*, and *c′* axes (where $c' = a \times b$) and match those reported earlier[4] and, as anticipated for monoclinic crystals, rotation about the *b* axis displayed no site-splitting. g-value measurements in the *ac′* plane showed that the previous EPR/ENDOR analysis was indeed conducted using a left-handed system. The right-handed g-tensor for copper-doped glycine is listed in Table 1. The right-handed tensors are related to those previously published by a sign change in each of the last three direction cosines.[20]

ENDOR data of Figures 1, 2, and 3 of Fujimoto et al.[4] were reanalyzed in the *abc′* reference system by a least-squares method using the spin Hamiltonian;

$$\mathscr{H} = \beta_e S \cdot g \cdot H + I \cdot A^N \cdot I + I \cdot \mathbf{Q}^N \cdot I - g_n^N \beta_n H \cdot I \quad (1)$$

Where $\mathbf{A}^N$, $\mathbf{Q}^N$, and g_n^N are the ^{14}N hyperfine tensor, traceless nuclear quadrupole tensor, and nuclear g-value, respectively, and the other quantities have their usual definition. ^{14}N ENDOR line assignments were made following a method applied by McDowell and Naito[8] to determine the relative signs of the ^{14}N hyperfine and quadrupole interactions. The refinement procedure has been described in previous work.[27] The angular dependencies of the ^{14}N ENDOR frequencies were correlated with those of the free proton frequency variations and also therefore with the g-tensor listed in Table 1. The newly refined ^{14}N hyperfine and quadrupole tensors reported in Table 1 are consistent with the ^{14}N coupling parameters found in the three other copper−amino acid crystal systems.

Quantum Mechanical Computations. Quantum mechanical calculations were carried out using the *Gaussian 03*[28] (G03) program. As mentioned above, the molecular structures and hyperfine couplings were calculated using DFT with the Becke 3-parameter exchange[29] and Lee−Yang−Parr correlation[30] functional. DFT computations using this functional have had relative success in estimating ^{14}N, ^{13}C, and ^{1}H hyperfine couplings in various copper model complexes.[23−25] The 3 by 3 hyperfine coupling tensor (**A**) for a particular nucleus (*n*) consists of the Fermi contact term (a_{iso}) and a electron spin-nuclear spin dipolar contribution ($A_{i,j}$), where $\mathbf{A} = a_{iso} + A_{i,j}$, with $i,j = x, y, z$, and were computed as implemented in G03 using the following relations:[31]

$$a_{iso} = \frac{4\pi}{3}\beta_e\beta_n g_e g_n \langle S_z \rangle^{-1} \rho_n^{\alpha-\beta} \quad (2)$$

where the spin density at the position of nucleus $\delta(r_n)$ is given by $\rho_n^{\alpha-\beta} = \sum_{u,v} P_{u,v}^{\alpha-\beta} \langle \phi_u | \delta(r_n) | \phi_v \rangle$, $P_{u,v}^{\alpha-\beta}$ are elements of the spin density matrix and the ϕ_κ's are the atomic basis which span the molecular orbitals, and

$$A_{i,j} = \beta_e\beta_n g_e g_n 2^{-1} \langle S_z \rangle^{-1} \sum_{u,v} P_{u,v}^{\alpha-\beta} \langle \varphi_u | r_n^{-5} (r_n^2 \delta_{i,j} - 3 r_{n,i} r_{n,j}) | \varphi_v \rangle \quad (3)$$

where other terms have their usual meaning. Spin−orbit coupling and higher order effects to the hyperfine couplings are neglected in the G03 compilations. Previous work has shown such effects to contribute only small corrections to calculated ligand couplings in copper systems.[24,25] Triple-ξ atomic basis plus polarization sets[32] (TZVP) supplied in G03 were used for all atoms in the QM computations that yielded the hyperfine couplings. Atomic basis of at least triple-ξ quality was recommended to be used for nitrogen and copper atoms in similar DFT calculations on copper−amino complexes.[24] Single-point energy QM computations of the systems in Figure 1 were performed using atomic coordinates from the most recent neutron diffraction results. Copper coordinates were determined according to descriptions in the EPR/ENDOR studies with the exception of alanine where Cu^{2+} was placed at the midpoint of the two coordinating oxygens. This only slightly repositioned the copper from the proposed site[8] and did not significantly alter the results. Also, the amino-bound hydrogens for triglycine sulfate and glycine were positioned according to single crystal ^{2}D ENDOR results as discussed below.

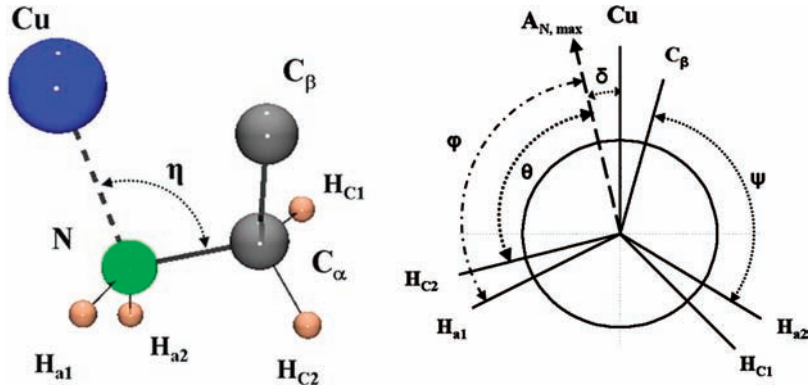

Figure 2. Left: Molecular fragment of copper bound to the amino group of glycine rendered by POV-RAY.[14] The Cu−N−C_α angle is η. H_{a1} and H_{a2} are the amino hydrogens and H_{C1} and H_{C2} are bound to C_α. Right: The molecular fragment on left looking down its C_α−N bond. The dashed $\mathbf{A}_{N,max}$ designates the projected direction of the maximum principal component of the ^{14}N hyperfine coupling tensor. Dihedral angles θ, φ, δ, and Ψ are defined as angles between planes $\mathbf{A}_{N,max}$−N−C_α and N−C_α−H_C, $\mathbf{A}_{N,max}$−N−C_α and C_α−N−H_a, Cu−N−C_α and C_α−N−$\mathbf{A}_{N,max}$, and H_a−N−C_α and N−C_α−C_β, respectively.

The present study focuses on ^{1}H couplings from hydrogens bound to the amino and adjacent carbon in copper−glycine systems. QM geometry optimizations of the crystalline copper−triglycine sulfate and copper−glycine complexes resulted in the axial ligand molecules to significantly shift toward the complex equatorial plane, forming strong hydrogen bonding interactions with the amino ligands. Because these optimized complexes had far different axial−equatorial interactions than those in the crystal structures, a simpler $Cu^{2+}(glycine)_2$ complex was deemed more suitable to theoretically model the ligand proton couplings. Geometric optimization of this gas-phase Cu^{2+}−glycine model was accomplished using the Berny algorithm,[33] employing a double-ξ plus polarization basis[34] (DGDZP) for all atoms. Previous application of similar double-ξ basis yielded acceptable geometries in similar compounds.[24,25] Atomic coordinates used to initiate the optimization procedure came from the neutron diffraction study of α-glycine. The final geometry of the $Cu^{2+}(glycine)_2$ model was similar to that shown in Figure 1 for the copper−glycine complex, excluding the two axial glycines. All G03 calculations of hyperfine couplings were performed using the NMR keyword and were done without symmetry constraints.

To the left in Figure 2 is displayed a molecular fragment of Cu-bound glycine. The Cu−N distance and Cu−N−C_α angle are designated as r and η, respectively. The protons of interest are H_a for the amino-bound and H_C for C_α-bound hydrogens. The right side of Figure 2 is a scheme that defines θ, φ, δ, and Ψ, the dihedral angles between the planes $\mathbf{A}_{N,max}$−N−C_α and N−C_α−H_C, $\mathbf{A}_{N,max}$−N−C_α and H_a−N−C_α, $\mathbf{A}_{N,max}$−N−C_α and Cu−N−C_α, and H_a−N−C_α and N−C_α−C_β respectively where $\mathbf{A}_{N,max}$ indicates the direction of the largest ^{14}N hyperfine tensor component. For the $Cu^{2+}(glycine)_2$ model, QM calculations were performed at different rotational orientations of the amino group about the C_α−N bond and at different dihedral angles between the Cu−N−C_α and N−C_α−C_β planes. The former causes changes in the φ angles for the two amino hydrogens. The latter introduces different θs for the C_α-bound hydrogens, and in addition, because the glycine structure beyond C_α is also displaced, geometric optimization of the model complex was again conducted at each dihedral angle setting. Hyperfine couplings were then determined for each newly optimized model geometry.

Results

Figure 3 illustrates plots of the copper binding to the amino group in the four crystal systems and in the $Cu^{2+}(glycine)_2$ model looking down the C_α−N bond. The projections of bonds and principal directions of the maximum ^{14}N hyperfine tensor component ($\mathbf{A}_{EXP}$ or $\mathbf{A}_{CAL}$) form the dihedral angles between various planes in the complexes. When copper binds, the amino groups lose a proton. Depending on the initial orientation of the leaving proton, the remaining protons may reorient about the C_α−N bond. In Figure 3, original amino H_a orientations are designated by the dashed bonds and the solid bonds are the proposed H_a (or ^{2}D) orientations. Previous nuclear quadrupole resonance studies have established a correlation between the direction of maximum quadrupole coupling in N−^{2}D and the bond direction.[35] Quadrupole coupling tensors from the ^{2}D ENDOR study of copper−triglycine sulfate were therefore used to locate the amino group ^{2}D atoms. Assuming hydrogens would undergo a reorientation similar to the deuterons, the amino hydrogens in the copper−triglycine complex were likewise positioned. Here, the N−H_a bond lengths were set to 1 Å. Comparing their rotational positions before and after copper binding, the triglycine sulfate amino hydrogens (denoted at D_{a1} and D_{a2}) rotated between 20−30° about the C_α−N from their original positions (H_{a2o} and H_{a3o}). These values are consistent with the 30° rotations reported in the ^{2}D ENDOR study.[6] Moreover, the close similarity between the original amino-group orientations of triglycine sulfate and glycine suggest a similar rotation for the glycine amino hydrogens. This similarity prompted an assumption in the present analysis that the original H_a hydrogens of glycine (denoted H_{a1o}, H_{a2o}, and H_{a2o}) rotate 20° about the C_α−N rotation when copper binds (H_{a1r}, H_{a2r}, and H_{a2r} in the site plot). This rotation causes a better alignment of the H_{a3} hydrogen (signified by the dashed bond) for its replacement by the copper ion. In glycylglycine and alanine, the relative closer correspondence between N−Cu and N−H_{a3} directions averts a significant rotation of the remaining two amino protons. However, for the alanine crystal complex, both the orientation of copper with respect to the N−C_α bond and the two nearly equivalent amino proton hyperfine couplings suggested a flattened amino group upon copper binding. The placements of the amino hydrogens in the flattened alanine were therefore estimated using the proton hyperfine tensor principal directions reported in the ENDOR study and are denoted $H_{a1/flat}$ and $H_{a2/flat}$, in the site plot.

The experimental ^{14}N maximum hyperfine direction ($\mathbf{A}_{EXP}$) is generally in close alignment with the N−Cu bond direction for all the complexes and is a good indicator of the projected orientation of the unpaired nitrogen p-orbital. In the corresponding QM calculations, the calculated nitrogen hyperfine maximum

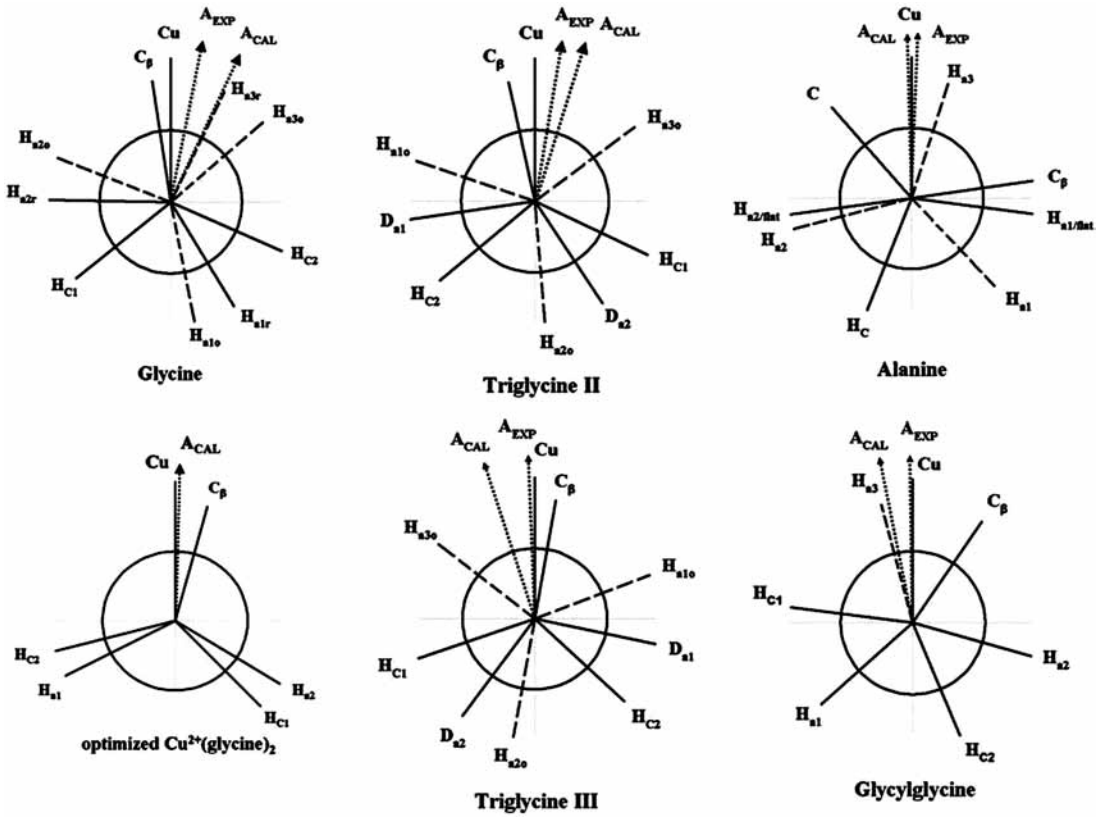

Figure 3. Copper site plots showing various projected directions looking down the $C_\alpha-N$ bonds of the crystal complexes and the geometry-optimized $Cu^{2+}(glycine)_2$ model. Directions were determined from crystallographic and ENDOR results for the four copper-doped crystals and from theoretical QM calculations of an optimized model. The original (dashed bonds) and rotated (or flattened) directions of amino-hydrogen bonds are labeled with subscripts. The dotted vectors $\mathbf{A}_{EXP}$ and $\mathbf{A}_{CAL}$ represent the experimental and QM calculated projected directions of the maximum ^{14}N hyperfine coupling components, respectively.

($\mathbf{A}_{CAL}$) directions have small but significant angular deviations ($\Delta\delta$) from the $\mathbf{A}_{EXP}$ directions and in all cases lies close to, but not exactly, the opposite bisector of the $H_{a1}-N-H_{a2}$ projected directions.

The bond and nitrogen hyperfine tensor directions in the site plots suggest the possibility for hyperconjugation as a means for the unpaired electron to transfer into the s-orbital of β-hydrogens. The amount of hyperconjugation in carbon free radicals having form $p-CH_2-CR_2-H$, where p refers to the carbon unpaired $p\pi$-orbital, follows the amount of orbital overlap of the carbon $p\pi$ and hydrogen 1s and therefore depends on the cosine-square of dihedral angle θ between the $p-C-C$ and $C-C-H$ planes.[36−38] This causes a systematic variation in ^1H isotropic hyperfine coupling according to the Heller-McConnell relation[36]

$$a_{iso} = \rho_\pi(B_o + B_2 \cos^2(\theta)), \quad (4)$$

where ρ_π is a measure of the spin density present in the $2p\pi$-orbital of the carbon, and B_o and B_2 are empirical constants.[36−38] A simplified representation of the copper−amino group complex is where the unpaired spin in the nitrogen 2p-orbital is mostly responsible for the ligand proton isotropic couplings. This would result in a similar type of a_{iso} dependence of the C_α hydrogen in the $p-N-C_\alpha-H_C$ moiety. For the $p-N-H_a$ fragment on the other hand, it is not clear whether the H_a couplings would exhibit any such systematic variation. To assess these possibilities, the relative dispositions of the $C_\alpha-H_C$ and $N-H_a$ bonds and unpaired nitrogen p-orbital directions with respect to the $C_\alpha-N$ bond, as well as the flattening of the amino group, were analyzed for their affect on the ligand ^1H a_{iso} values. The contribution of the copper unpaired orbital to the ligand nitrogen hyperfine couplings has been estimated to be less than 10%.[24] Because the amino and C_α hydrogens are in a near eclipsed arrangement on the other side of the amino moiety (Figure 2), the copper orbital contributions to the proton isotropic hyperfine couplings were assumed to be small in the present analysis.

Table 2 lists the experimental and QM calculated ^{14}N hyperfine coupling parameters derived from the tensor quantities. These are $\mathbf{A}_+ = A_{max} - a_{iso}$ and $\mathbf{A}_- = A_{min} - a_{iso}$, where A_{max} and A_{min} are the maximum and minimum ^{14}N hyperfine couplings, respectively. Also listed are the Cu−N distance (r) and $Cu-N-C_\alpha$ angle (η) for each complex. The experimental distance r varies from a short value of 1.768 Å found in glycine to 2.181 Å in glyclglycine, and although none conform to the optimized copper−glycine model value of 2.042 Å, these are still within the range of bond lengths found for crystals.[39] The η for the proposed flattened alanine is near 90°, glycylglycine has a value of 98°, and both glycine systems are close to the 108° found for the gas phase optimized copper−glycine model. The anisotropies of the experimental ^{14}N hyperfine tensors are similar and are close to axial, having an average total anisotropy ($\mathbf{A}_+ - \mathbf{A}_-$) of 13.23 MHz, except for the alanine complex, which has a higher value of 14.85 MHz. The isotropic coupling for copper−alanine is also larger (32.13 MHz) than the average found in the other systems (24.95 MHz). Overall, the QM computed anisotropic tensor components have general agreement with the corresponding experimental values, whereas the isotropic couplings have somewhat larger deviations. Calculations also show that a flattening of the alanine amino group significantly decreases the ^{14}N isotropic coupling while

TABLE 2: Geometric (*r*: Cu−N, η: Cu−N−C_α) and ^{14}N Hyperfine Coupling Parameters (A_+, A_-, a_{iso} in MHz, where $A_+ = A_{max} - a_{iso}$, $A_- = A_{min} - a_{iso}$ and A_{max} and A_{min} Are the maximum and Minimum ^{14}N Hyperfine Values, Respectively) for Coordinated Amino Nitrogen Determined from Published Crystallographic Parameters, ENDOR Measurements and QM Calculations (*Parentheses*) for Proposed Sites in copper-Doped Amino Acid Crystals and for Geometry-Optimized Cu(glycine)$_2$

	nitrogen	r (Å)	η (°)	A_+	A_-	a_{iso}
alanine						
	amino N	2.109	90.3	9.79 *(10.40)*	−5.06 *(−5.23)*	32.13 *(10.25)*
glycine						
	amino N	1.768	113.5	7.80 *(7.62)*	−4.02 *(−3.97)*	24.64 *(23.97)*
triglycine sulfate						
	amino NII	1.890	110.8	8.60 *(5.98)*	−5.10 *(−3.04)*	23.50 *(30.72)*
	amino NIII	1.940	111.6	8.73 *(7.70)*	−5.17 *(−3.86)*	24.07 *(35.77)*
glycyl-glycine						
	amino N	2.181	97.5	7.53 *(8.02)*	−4.37 *(−4.06)*	27.57 *(31.46)*
Cu^{2+}(glycine)$_2$optimized geometry						
	amino N	*(2.042)*	*(108.0)*	*(9.37)*	*(−4.71)*	*(38.07)*

increasing its anisotropy, which is inconsistent with the observation. Figure 4 is a plot of the dependence of the anisotropic parameters A_+ and A_- as a function of a_{iso} for both experimental and calculated ^{14}N tensors, including results for the geometric-optimized Cu^{2+}(glycine)$_2$ model. Besides a smaller overall anisotropy of 11.56 MHz calculated for molecule III of triglycine sulfate, and higher value of 15.63 MHz for alanine and slightly higher (14.08 MHz) for the copper−glycine model, the ^{14}N hyperfine anisotropy remains relatively constant with an overall average of 12.33 MHz and an experimental average value of 13.23 MHz, indicating a nearly equivalent nitrogen p-orbital spin density in the crystal complexes and optimized model.

Table 3 reports the experimental and QM computed (in parentheses) proton hyperfine coupling parameters; $A_+ = A_{max} - a_{iso}$ and $A_- = A_{min} - a_{iso}$ (where A_{max}, A_{min}, and a_{iso} are the maximum, minimum, and isotropic ^1H hyperfine couplings, respectively), for both the amino and C_α-bound hydrogens. Also listed are the dihedral angles between the hydrogens and the nitrogen A_{EXP} or A_{CAL} directions. The C_α−N−A_{EXP} and C_α−N−A_{CAL} planes are both found to slightly deviate from Cu−N−C_α with δ ranging from a low of 1° for alanine to a high of 15° for molecule III of trigylcine sulfate. However, there is no apparent correlation between the magnitude of δ and how well the calculated proton couplings agree with the observed values. The agreement is far better for some protons than for others. Figure 5 plots the proton anisotropic parameters A_+ and A_- versus isotropic coupling a_{iso} for the copper complexes as well as for the optimized copper−glycine model taken from Table 3. Similar plots have been useful in the past to categorize proton couplings in free radicals.[40] Figure 5 shows that when a_{iso} becomes more positive the total hyperfine anisotropy decreases by ∼20%, from 6.8 to 5.2 MHz for the C_α-bound hydrogens (part a of Figure 5) and from 21 to 16 MHz for the amino hydrogens (part b of Figure 5), signifying only a small increase in effective distance between unpaired spin and proton occurs. The large total anisotropy of 11.84 MHz observed for the H_{C1} of glycylglycine in part a of Figure 5 is anomalous and could be a consequence of its closer proximity to the copper than the other hydrogens. Also, for both the C_α-bound and amino hydrogens, the anisotropic hyperfine parameters calculated for the flattened alanine (open triangles) are smaller than for the general trend of the data.

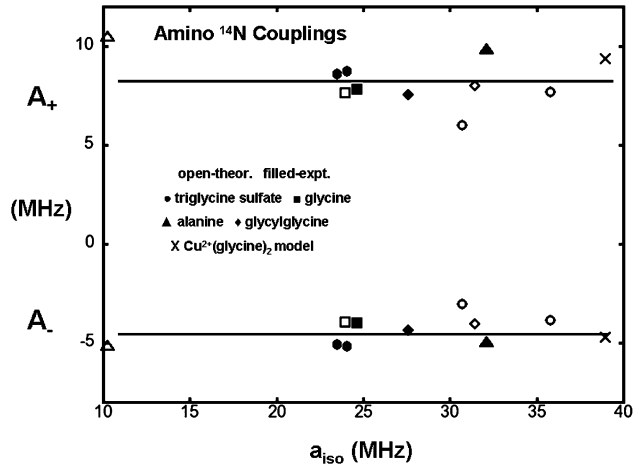

Figure 4. Plot of the amino ^{14}N hyperfine anisotropic hyperfine parameters A_+ and A_- as a function of the isotropic hyperfine coupling a_{iso}. Here, $A_+ = A_{max} - a_{iso}$ and $A_- = A_{min} - a_{iso}$, where A_{max} and A_{min} are the maximum and minimum values of the ^{14}N hyperfine coupling tensor, respectively. Data are taken from Table 2. The filled symbols are from ENDOR measurements for the four copper-doped crystals and the open symbols are results from theoretical QM hyperfine calculations of the copper complexes in Figure 3 and for the geometrically optimized Cu^{2+}(glycine)$_2$ model (X).

The proton a_{iso}'s of the C_α-bound hydrogens in Table 3 are plotted as a function of dihedral angle θ. This angle represents either the angle between the A_{EXP}−N−C_α and N−C_α−H_C planes for the experimental couplings or between the A_{CAL}−N−C_α and H_a−N−C_α planes for the QM calculated couplings. The results are displayed in Figure 6. The solid line represents a best fit curve for the observed couplings with $a_{iso} = -1.0_9(4_0) + 8.2_1(8_2)\cos^2(\theta)$ MHz. The observed alanine coupling values lie near the curve but were not included in the fit because it was not known whether a flattened amino geometry would demonstrate the same cosine-square parameters as a pyramidal one. Previous EPR and ENDOR studies on bent (pyramidal) carbon free radical systems have measured smaller β-proton a_{iso}'s as compared to the flattened radicals, which was attributed to a reduction in $\rho_\pi B_2$.[41−44] The open symbols represent calculated couplings and show marked deviations from the experimental values at high dihedral angles. The dashed line traces out the variation in calculated a_{iso} values for the copper−glycine model which was geometry-optimized at each specific dihedral angle. This line is actually a composite of two near identical lines, one from each of the two H_C's. The values calculated for the unrestricted geometry-optimized Cu^{2+}(glycine)$_2$ are shown as X's and lie on the dashed curve. The calculated nitrogen hyperfine isotropic coupling (37.7 MHz ± 3%) and total anisotropy (14.2 MHz ± 1%) remain roughly constant over the

TABLE 3: Angular (δ, θ, φ) and ^{1}H Hyperfine Coupling Parameters (A_+, A_-, a_{iso} in MHz, where $A_+ = A_{max} - a_{iso}$, $A_- = A_{min} - a_{iso}$ and A_{max} and A_{min} Are the Maximum and Minimum ^{1}H Hyperfine Values, Respectively) for the Amino N−H_a and C_α−H_C Hydrogens Determined from Published Crystallographic Parameters, ENDOR Measurements, and QM Calculations *(Parentheses)* of Copper-Doped Amino Acid Crystals[a]

system	δ	hydrogen	θ	φ	A_+	A_-	a_{iso}
alanine	2.4 *(1.0)*						
		Hc_1	161		3.20	−2.11	5.47
			(158)		*(1.37)*	*(−1.49)*	*(6.01)*
		H_{a1}		95	10.6	−8.69	−5.31
				(98)	*(7.52)*	*(−6.67)*	*(−8.00)*
		H_{a2}		100	11.0	−8.28	−5.82
				(97)	*(7.66)*	*(−6.50)*	*(−7.58)*
glycine	12.5 *(26.2)*						
		H_{C1}	141		3.19	−2.02	3.16
			(155)		*(3.20)*	*(−2.04)*	*(6.82)*
		H_{C2}	101		not detected		
			(88)		*(3.64)*	*(−2.08)*	*(−0.13)*
		H_{a1}		136	9.66	−7.57	−3.53
				(123)	*(10.1)*	*(−7.33)*	*(−1.47)*
		H_{a2}		101	11.0	−7.59	−6.31
				(115)	*(15.4)*	*(−10.8)*	*(−7.70)*
triglycine sulfate	8.3 *(17.0)* 1.9 *(17.1)*						
		H_{C1}	108		4.36	−2.44	0.08
			(99)		*(3.25)*	*(−1.89)*	*(−0.40)*
		H_{C2}	139		3.52	−2.02	3.75
			(148)		*(2.90)*	*(−1.86)*	*(4.07)*
		H_{a1}		107	11.2	−8.10	−5.70
				(116)	*(11.4)*	*(−7.67)*	*(−5.87)*
		H_{a2}		139	10.7	−8.10	−4.05
				(131)	*(9.43)*	*(−6.62)*	*(−0.42)*
		$H_{C1'}$	107		4.28	−2.37	0.07
			(92)		*(3.65)*	*(−2.05)*	*(−0.38)*
		$H_{C2'}$	135		3.28	−1.86	3.65
			(151)		*(3.34)*	*(−2.36)*	*(2.79)*
		$H_{a1'}$		104	10.8	−7.75	−5.75
				(119)	*(11.9)*	*(−8.78)*	*(−6.41)*
		$H_{a2'}$		142	10.1	−7.55	−3.75
				(127)	*(10.8)*	*(−7.87)*	*(−1.98)*
glycyl-glycine	0.7 *(11.2)*						
		H_{C1}	82		6.73	−5.11	−1.83
			(72)		*(4.10)*	*(−2.36)*	*(0.67)*
		H_{C2}	158		3.06	−1.97	5.91
			(169)		*(2.74)*	*(−1.79)*	*(4.10)*
		H_{a1}		131	not measured		
				(121)	*(8.64)*	*(−6.70)*	*(−3.03)*
		H_{a2}		107	not measured		
				(117)	*(8.80)*	*(−6.81)*	*(−4.43)*
optimized-geometry $Cu^{2+}(glycine)_2$	*(1.4)*						
		H_{C1}	*(138)*		*(2.85)*	*(−1.88)*	*(3.22)*
		H_{C2}	*(103)*		*(3.39)*	*(−1.98)*	*(0.31)*
		H_{a1}	*(121)*		*(10.7)*	*(−8.29)*	*(−5.92)*
		H_{a2}	*(119)*		*(10.9)*	*(−8.14)*	*(−6.27)*

[a] The dihedral angles δ, θ, and φ (°) are defined in Figure 2.

range of dihedral angles. The model a_{iso} variation gives a maximum near 155° and declines at higher dihedral angle. This result is unexpected for a simple hyperconjugation transfer of spin density, which should produce maximum isotropic couplings at dihedral angles of 0° and 180°. Similar a_{iso} variations with dihedral angle were obtained from computations employing different atomic basis sets; 6-311G, DGDVP, or EPR-III, in G03.[28] Previous INDO calculations of pyramidal-shaped carbon free radicals indicate asymmetries in their β-proton $\cos^2\theta$ curves having different a_{iso} maximum values occurring at 0 and 180°,[42−44] owing presumably to the different spin density distributions of the orbital lobes on either side of the carbon.[42] To assess whether such a pyramidal shaped amino group causes the declining trend in Figure 6, QM calculations were conducted on a series of copper−glycine models at various θ dihedral angles with the C_α−NH_2 amino group flattened into a planar geometry. Here too, the a_{iso} variation curve gave a similar pattern. This consistency suggests that the DFT/B3LYP calculations predict a more complicated mechanism for spin transfer onto the C_α hydrogens.

Figure 7 shows the variation of amino proton a_{iso}'s with dihedral angle φ, the angle between planes $\mathbf{A}_{EXP}$−N−C_α and C_α−N−H_a for the observed couplings, or between planes $\mathbf{A}_{CAL}$−N−C_α and H_a−N−C_α for the QM calculated couplings. As this angle approaches 180°, the nitrogen unpaired p-orbital should increase its overlap with the H_a s-orbital. This is consistent with the observed couplings. The solid line represents a good fit to the experimental isotropic values with a_{iso} =

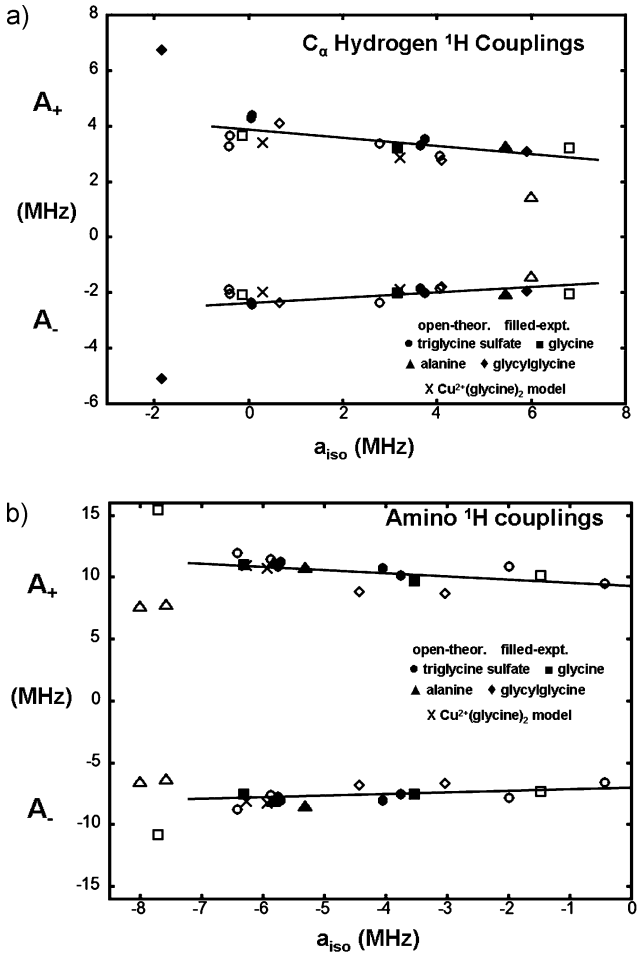

Figure 5. Plots of the (a) C_α-bound hydrogen and (b) amino-bound hydrogen ^{1}H hyperfine anisotropic hyperfine parameters $\mathbf{A}_+$ and $\mathbf{A}_-$ as a function of the isotropic hyperfine coupling a_{iso}. Here, $\mathbf{A}_+ = A_{max} - a_{iso}$ and $\mathbf{A}_- = A_{min} - a_{iso}$, where A_{max} and A_{min} are the maximum and minimum value of the ^{1}H hyperfine coupling tensor, respectively. Data are taken from Table 3. The filled symbols are from the ENDOR measurements on the four copper-doped crystals and the open symbols are results from theoretical QM calculations from the copper-complexes in Figure 3 and from the geometrically-optimized $Cu^{2+}(glycine)_2$ model (X).

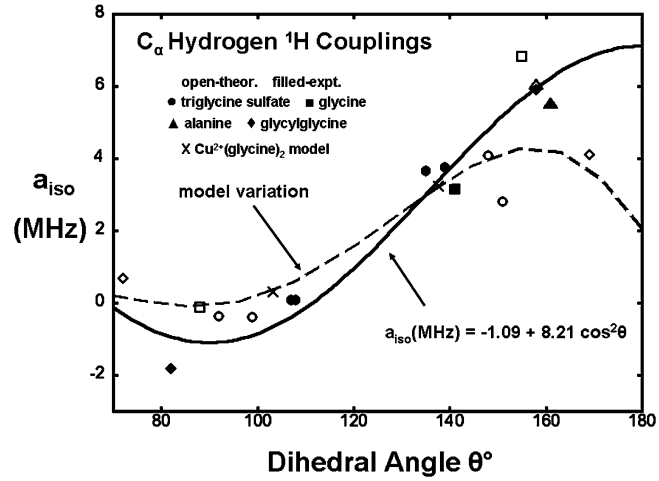

Figure 6. Plot of the C_α-bound hydrogen ^{1}H isotropic hyperfine coupling a_{iso} as a function of the $\mathbf{A}_{EXP}-N-C_\alpha-H_C$ (or $\mathbf{A}_{CAL}-N-C_\alpha-H_C$) dihedral angle θ. Data was taken from Table 3. The filled symbols are from ENDOR measurements of the four copper-doped crystals and the open symbols are results of theoretical QM calculations from the copper complexes in Figure 3 and from the geometrically optimized $Cu^{2+}(glycine)_2$ model (X). The experimental data were fit to $a_{iso} = -1.0_9(4_0) + 8.2_1(8_2)\cos^2\theta$ MHz shown by the solid line curve. The two dashed overlapping lines (one for each H_C) trace out the variation in the QM calculated ^{1}H isotropic couplings in $Cu^{2+}(glycine)_2$ geometry-optimized models at fixed θ dihedral angles.

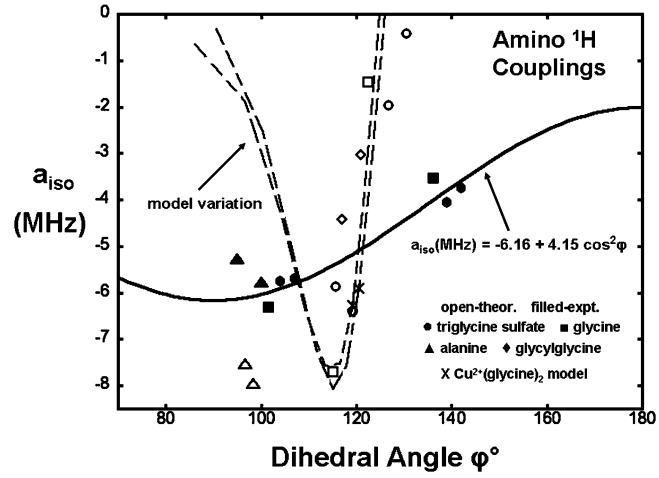

Figure 7. Plot of the amino group hydrogen isotropic hyperfine coupling a_{iso} as a function of the dihedral angle φ between the $\mathbf{A}_{EXP}-N-C_\alpha$ (or $\mathbf{A}_{CAL}-N-C_\alpha$) and H_a-N-C_α planes. Data was taken from Table 3. The filled symbols are from ENDOR measurements of three of the four copper-doped crystals and the open symbols are results of theoretical QM calculations from the copper-complexes in Figure 3 and from the geometrically optimized $Cu^{2+}(glycine)_2$ model (X). The experimental data were fit to $a_{iso} = -6.1_6(2_2) + 4.1_5(5_3)\cos^2\varphi$ MHz shown by the solid line curve. The slightly different dashed lines (one for each amino H_a) trace out the variation in the QM calculated couplings for the geometry-optimized $Cu^{2+}(glycine)_2$ model as the $C_\alpha-N$ bond was incrementally rotated. This rotation changed the φ dihedral angle by specific amounts.

$-6.1_6(2_2) + 4.1_5(5_3)\cos^2\varphi$ MHz. Again, even though the alanine couplings appear to fall on the fit curve, its amino hydrogen a_{iso}'s were not included in the fit. The near equivalence of the alanine amino proton couplings, both observed (filled triangles) and calculated (open triangles), agrees with the nitrogen $2p\pi$-orbit symmetry in a flattened amino group. In marked contrast, the calculated a_{iso}'s for the other complexes deviate significantly from the observed values. The two slightly different dashed lines in Figure 7 trace the QM calculated a_{iso} for each amino H_a as the $C_\alpha-N$ bond was rotated in the geometry-optimized $Cu^{2+}(glycine)_2$ model. The slightly different lines are due to the asymmetry of the site. The calculated ^{14}N hyperfine isotropic coupling (39.3 MHz ± 5%) and total anisotropy (13.6 MHz ± 5%) have relatively small variations over this range of dihedral angles and cannot therefore account for the steep dependence shown in this curve. The model and experimental ^{1}H a_{iso} variation curves are very different, having only two small common regions near 105 and 120°. One of these falls near the geometrically optimized model values of $\varphi = 119$ and 121° for $a_{iso} = -6.27$ and -5.92 MHz, respectively (shown as X's on the dashed line). The sharpest minimum in the calculated model variation curve happens when $C_\alpha-C_\beta$ eclipses $\mathbf{A}_{CAL}$. This configuration also corresponds to a sharp turnaround in the magnitude of the C_β Mulliken spin density. It is possible that changes in C_β unpaired spin density could indirectly affect the calculated isotropic couplings of the amino hydrogens by transferring some spin onto C_α. Overall, the theoretical proton a_{iso}'s for the crystal complexes agree much better with the model variation than with the experimental a_{iso}'s. In general, the extreme geometric sensitivity exhibited by the model variation

for the amino hydrogen isotropic couplings is incompatible with the experimental findings.

Discussion

The experimental hyperfine isotropic couplings for the amino hydrogens in the copper-doped crystal complexes depend on the dihedral angle φ between the nitrogen p-orbital and the N−H_a bond, according to $a_{iso} = -6.16 + 4.15 \cos^2\varphi$ MHz (Figure 7). It must be noted that the angular range over which this fit takes place is quite limited (about 45°) but this may also span the physically relevant geometries for copper coordinated amino acids. Also, the geometric variation of spin density on these hydrogens cannot really be ascribed to hyperconjugation simply because they are bound directly to the central atom (nitrogen) that bears the pπ spin density. On the other hand, the observed trend is consistent with a systematic change in the amount of hydrogen s contribution to the unpaired wave function. Similar empirical relationships have been proposed for V=O complexes and are useful predictors of metal coordination geometry.[45,46] Clearly, for the present systems, the QM calculations do not support the observed trend and instead demonstrate a very large geometric sensitivity of the proton isotropic coupling as the nitrogen p-orbital direction changes relative to the N−H_a bond. As remarked above, some of this sensitivity may arise from indirect effects caused by spin density delocalized on C_β, and this remains a point for further investigation.

If one of the H_a's is oriented in the nodal plane of the nitrogen unpaired p-orbital, that is, with $\varphi = 90°$, the empirical formula in Figure 7 gives an a_{iso} of −6.16 MHz. The structure of the oriented p−N−H_a resembles a planar nitrogen radical, permitting the application of the McConnell relationship[47] $a_{iso} = Q\rho_\pi$, where constant Q is proportional to the amount of spin polarization of the hydrogen 1s orbital, to calculate the spin density in the nitrogen 2pπ-orbital. With a_{iso}= −6.16 MHz and using a Q of −81 MHz found for nitrogen free radicals,[48] one finds $\rho_\pi \approx 0.076$ for the amino nitrogen. This is somewhat lower than the spin density $\rho_\pi \approx 0.094$ determined using the ratio of the observed nitrogen hyperfine anisotropy (average total value = 13.23 MHz) to the anisotropy calculated for the nitrogen valence p-state self-consistent wave function (141 MHz).[38] However, the latter ρ_π should be reduced by ∼10% to take into account the copper unpaired orbital contribution to the nitrogen hyperfine anisotropy.[24] Both ρ_π values fall within the range of nitrogen spin densities determined by a previous QM/DFT study of ligand hyperfine couplings in similar copper−nitrogen systems.[24]

The experimental data in Figure 6 fit a Heller-McConnell cosine-square function of the form $a_{iso} = -1.09 + 8.21 \cos^2\theta$ MHz, and suggests a hyperconjugative-like mechanism for the direct transfer of spin density from the amino nitrogen to the β-positioned C_α hydrogens. To test the derived B_0 and B_2 quantities, a comparison was made with ^{1}H isotropic couplings measured by ENDOR on trinitrophenylmethylnitroxide,[49] a nitroxyl radical which contains a rotating methyl group bound to the nitrogen, which carries significant π spin density. If the methyl group rotates rapidly, then an average isotropic hyperfine coupling $\langle a_{iso}\rangle$ is observed for each β-proton, where $\langle a_{iso}\rangle = \rho_\pi(B_0 + (^1/_2)B_2)$, and ρ_π is the spin in the nitrogen 2pπ-orbital.[37] Spin density is equally shared between the oxygen and nitrogen 2pπ-orbitals of the nitroxyl. This gives $\rho_\pi \approx 0.5$ for the nitrogen p-orbital. The single crystal ENDOR analysis finds $\langle a_{iso}\rangle = 29.5$ MHz for the rotating methyl group hydrogens, which in turn gives $(B_0 + (^1/_2)B_2) \approx 59$ MHz. Using the fit B_0 and B_2 parameters in Figure 6 and a nitrogen spin density of 0.076 from above, $(B_0 + (^1/_2)B_2) \approx 40$ MHz for the C_α hydrogens, which is somewhat smaller than that for trinitrophenylmethylnitroxide. However, allowing for the small number of available data and the difference between a nitroxyl radical and a copper-coordinated amino group, the parameters in Figures 6 and 7 for the cosine-square relationships are very reasonable.

The two empirical formulas found above are also consistent with results reported by pulsed-EPR/ENDOR studies of Cu^{2+}-histidine in frozen solution, which measured and analyzed the proton hyperfine parameters in a bis-histamine coordination complex.[25,50] This study reports a_{iso} values of −10 and −9 MHz for the two amino hydrogens, and 10.9 MHz for the alpha-carbon hydrogen. Although the magnitudes of these three couplings exceed the maximum values predicted by the empirical formulas above, this can be explained if the complex possessed a larger amino nitrogen pπ spin density than for the present systems. The present results would then suggest that the H_a's of Cu^{2+}-histidine have similar φ angles (near 120°) and predicts a $\mathbf{A}_{N,max}$−N−C_α−H dihedral angle of ∼160°. The latter supports the author's conclusion, based on the their analysis of the proton anisotropic hyperfine parameters, that the C_α−H bond is directed significantly away from the copper.[25,50] Unfortunately, this cannot be evaluated because the coordinated nitrogen hyperfine couplings for the Cu^{2+}−histidine complex have yet to be measured and analyzed.

Conclusion

Experimental values of amino-bound and C_α-bound proton isotropic hyperfine couplings in copper-amino acid complexes were found to empirically depend on the cosine-square of dihedral angles containing the nitrogen p-orbital and the hydrogen atoms. The C_α-bound hydrogen couplings varied according to $a_{iso} = -1.09 + 8.21 \cos^2\theta$ MHz (Figure 6), and the amino hydrogen couplings varied as $a_{iso} = -6.16 + 4.15 \cos^2\varphi$ MHz (Figure 7). The geometry of the p−N−C_α−H moiety would further suggest a hyperconjugative-like mechanism for transfer of spin density from nitrogen into the C_α-hydrogen s-orbital. For the amino-bound hydrogens, the mechanism for spin transfer is likely to be more complicated.

Results from the DFT quantum mechanical calculations gave mixed agreement with the experimental data. The hyperfine anisotropies calculated for both ^{14}N and ^{1}H couplings had much better correspondence with experimental trends than the isotropic couplings. The angular dependency of the proton isotropic hyperfine coupling computed by DFT only partially modeled the variation observed for the C_α hydrogens and failed to model the amino hydrogens. Although there appears to be some correlation with the amount of spin delocalized on C_β and the extreme geometric sensitivity of the a_{iso}'s for the amino hydrogens, no simple explanation can be devised. The theoretical findings also failed to match successes found by previous QM/DFT studies on vanadyl−water and vanadyl−imidazole complexes.[45,46] In these and earlier studies, water hydrogen and imidazole nitrogen couplings were found to experimentally depend on the dihedral angle containing the vanadyl unpaired d-orbital and the O−H bond for the water complex[45] or the coordinated nitrogen pπ-orbital direction for the imidazole complex.[51] These variations were subsequently found to be in very good agreement with those theoretically determined.[45,46] Apparently for copper−amino acid systems, the subtle balance of unpaired electron spin on Cu, N, C_α, and possibly C_β has significant influence on the theoretically computed proton hyperfine couplings. In addition, the difficulty in being able to accurately model small ligand hyperfine couplings using DFT has been discussed in recent studies.[23−25] Nevertheless, the deduced empirical spatial−spectral relationships found in the

current work will be useful in revealing bonding aspects found from EPR studies of similar complexes and improves our understanding of spin delocalization in copper−amino acid complexes and will help in interpreting proton hyperfine couplings in biological systems.

Acknowledgment. We thank SUNY/Old Westbury student Ms. Kacey-Ann Thompson for her help in the early stages of the crystallographic analysis. The following grants are acknowledged for financial support: NIGMS 5S06GM008180 (to M.J.C.), NIGMS GM071512 (to J.V.), and U.S. Public Health Service Grant GM40168 (to J.P.).

Supporting Information Available: Pictorial views of the singly occupied molecular orbital (SOMO) and spin density calculated for the geometry optimized $Cu^{2+}(glycine)_2$ model and for this model with one of the CN bonds rotated by 40°. This material is available free of charge via the Internet at http://pubs.acs.org.

References and Notes

(1) Abragam, A.; Bleany, B. *Electron Paramagnetic Resonance of Transition Ions*; Clarendon: Oxford, 1970.

(2) Steren, C. A.; Calvo, R.; Piro, O. E.; Rivero, B. E. *Inorg. Chem.* **1989**, *28*, 1933. (a) Dalsto, S. D.; Ferreyra, M. G.; Calvo, R.; Piro, O. E.; Castellano, E. E. *J. Inorg. Biochem.* **1999**, *73*, 151.

(3) Windsch, W.; Weltner, M. *Z. Naturforsch.* **1967**, *22a*, 1. (a) Stankowski, J. *Acta Phys. Pol.* **1968**, *33*, 387. (b) Fujimoto, M.; Janecka, J. *J. Chem. Phys.* **1971**, *55*, 1152. (c) Hirasawa, R.; Kon, H. *J. Chem. Phys.* **1972**, *56*, 4467. (d) Fujimoto, M.; Wylie, L. A.; Saito, S. *J. Chem. Phys.* **1973**, *58*, 1273.

(4) Fujimoto, M.; McDowell, C. A.; Takui, T. *J. Chem. Phys.* **1979**, *70*, 3694.

(5) Böttcher, R.; Heinhold, D.; Windsch, W. *Chem. Phys. Let.* **1977**, *49*, 148. (a) Böttcher, R.; Heinhold, D.; Wartewig, S.; Windsch, W. *J. Mol. Struct.* **1978**, *46*, 363. (b) Fujimoto, M.; McDowell, C. A.; Takui, T. *J. Chem. Phys.* **1979**, *70*, 3694. (c) Wartewig, S.; Böttcher, R.; Windsch, W. *Chem. Phys.* **1981**, *58*, 211. (d) Böttcher, R.; Metz, H.; Windsch, W. *J. Mol. Struct.* **1982**, *83*, 31. (e) Böttcher, R.; Metz, H.; Windsch, W. *Chem. Phys.* **1985**, *93*, 137.

(6) Böttcher, R.; Heinhold, D.; Windsch, W. *Chem. Phys.* **1985**, *93*, 339.

(7) Calvo, R.; Oseroff, S. B.; Abache, H. C. *J. Chem. Phys.* **1980**, *72*, 760.

(8) McDowell, C. A.; Naito, A. *J. Magn. Reson.* **1981**, *45*, 205.

(9) McDowell, C. A.; Naito, A.; Sastry, D. L.; Cui, Y.; Sha, K. *J. Phys. Chem.* **1990**, *94*, 8113.

(10) McDowell, C. A.; Naito, A.; Sastry, D. L.; Cui, Y.; Sha, K.; Yu, S. X. *Mol. Struct.* **1989**, *185*, 361.

(11) Slutter, C. E.; Gromov, I.; Epel, B.; Pecht, I.; Richards, J. H.; Goldfarb, D. *J. Am. Chem. Soc.* **2001**, *123*, 5325.

(12) Aronoff-Spencer, E.; Burns, C. S.; Avdievich, N. I.; Gerfen, G. J.; Peisach, J.; Antholine, W. E.; Ball, H. L.; Cohen, F. E.; Prusiner, S. B.; Millhauser, G. L. *Biochemistry* **2000**, *39*, 13760. (a) Van Doorslaer, S.; Cereghetti, G. M.; Glockshuber, R.; Schweiger, A. *J. Phys. Chem. B* **2001**, *105*, 1631. (b) Burns, C. S.; Aronoff-Spencer, E.; Dunham, C. M.; Lario, P.; Avdievich, N. I.; Antholine, W. E.; Olmstead, M. M.; Vrielink, A.; Gerfen, G. J.; Peisach, J.; Scott, W. G.; Millhauser, G. L. *Biochemistry* **2002**, *41*, 3991. (c) Burns, C. S.; Aronoff-Spencer, E.; Legname, G.; Prusiner, S. B.; Antholine, W. E.; Gerfen, G. J.; Peisach, J.; Millhauser, G. L. *Biochemistry* **2003**, *42*, 6794. (d) Chattopadhyay, M.; Walter, E. D.; Newell, D. J.; Jackson, P. J.; Aronoff-Spencer, E.; Peisach, J.; Gerfen, G. J.; Bennett, B.; Antholine, W. E.; Millhauser, G. L. *J. Am. Chem. Soc.* **2005**, *127*, 12647. (e) Colombo, M. C.; VandeVondele, J.; Van Doorslaer, S.; Laio, A.; Guidoni, L.; Rothlisberger, U. *Proteins: Struct., Funct., Bioinf.* **2008**, *70*, 1084.

(13) Farrugia, L. J. *J. Appl. Crystallogr.* **1997**, *30*, 565.

(14) http://www.povray.org; Persistence of Vision Raytracer Pty. Ltd., **2006**.

(15) Jönsson, P-G. Kvick, Å. *Acta Crystallogr.* **1972**, *B28*, 1827.

(16) Kay, M. I.; Kleinberg, R. *Ferroelectrics* **1973**, *5*, 45.

(17) Lehmann, M. S.; Koetzle, T. F.; Hamilton, W. C. *J. Am. Chem. Soc.* **1972**, *94*, 2657.

(18) Kvick, Å.; Al-Karaghouli, A. R.; Koetzle, T. F. *Acta Crystallogr.* **1977**, *B33*, 3796. (a) Kvick, Å.; Koetzle, T. F.; Stevens, E. D. *J. Chem. Phys.* **1979**, *71*, 173.

(19) Peisach, J.; Blumberg, W. E. *Arch. Biochem. Biophys.* **1974**, *165*, 691.

(20) Gordy, W. *Theory and Application of Electron Spin Resonance*; John Wiley & Sons: New York, 1980.

(21) Hohenberg, P.; Kohn, W. *Phys. Rev. B* **1964**, *864*, 136. (a) Kohn, W.; Sham, L. J. *Phys. Rev. A* **1965**, *140*, 1133.

(22) Parr, R. G.; Yang, W. *Density Functional Theory of Atoms and Molecules*; Oxford University Press: New York, 1989. (a) Chong, D. P. *Recent Advances in Density Functional Methods Part 1*; World Scientific Publishing: Singapore, 1995.

(23) Munzarová, M.; Kaupp, M. *J. Phys. Chem.* **1999**, *103*, 9966.

(24) Neese, F. *J. Phys. Chem.* **2001**, *105*, 4290.

(25) Baute, D.; Arieli, D.; Neese, F.; Zimmermann, H.; Weckhuysen, B. M.; Goldfarb, D. *J. Am. Chem. Soc.* **2004**, *126*, 11733.

(26) McDowell, C. A.; Fujimoto, M. Personal communication.

(27) Colaneri, M.; Peisach, J. *J. Am. Chem. Soc.* **1995**, *117*, 6308.

(28) Frisch, M. J.; Trucks, G. W.; Schlegel, H. B.; Scuseria, G. E.; Robb, M. A.; Cheeseman, J. R.; Montgomery, J. A., Jr.; Vreven, T.; Kudin, K. N.; Burant, J. C.; Millam, J. M.; Iyengar, S. S.; Tomasi, J.; Barone, V.; Mennucci, B.; Cossi, M.; Scalmani, G.; Rega, N.; Petersson, G. A.; Nakatsuji, H.; Hada, M.; Ehara, M.; Toyota, K.; Fukuda, R.; Hasegawa, J.; Ishida, M.; Nakajima, T.; Honda, Y.; Kitao, O.; Nakai, H.; Klene, M.; Li, X.; Knox, J. E.; Hratchian, H. P.; Cross, J. B.; Bakken, V.; Adamo, C.; Jaramillo, J.; Gomperts, R.; Stratmann, R. E.; Yazyev, O.; Austin, A. J.; Cammi, R.; Pomelli, C.; Ochterski, J. W.; Ayala, P. Y.; Morokuma, K.; Voth, G. A.; Salvador, P.; Dannenberg, J. J.; Zakrzewski, V. G.; Dapprich, S.; Daniels, A. D.; Strain, M. C.; Farkas, O.; Malick, D. K.; Rabuck, A. D.; Raghavachari, K.; Foresman, J. B.; Ortiz, J. V.; Cui, Q.; Baboul, A. G.; Clifford, S.; Cioslowski, J.; Stefanov, B. B.; Liu, G.; Liashenko, A.; Piskorz, P.; Komaromi, I.; Martin, R. L.; Fox, D. J.; Keith, T.; Al-Laham, M. A.; Peng, C. Y.; Nanayakkara, A.; Challacombe, M.; Gill, P. M. W.; Johnson, B.; Chen, W.; Wong, M. W.; Gonzalez, C.; Pople, J. A. *Gaussian 03, revision E.01*; Gaussian, Inc.: Wallingford, CT, 2007.

(29) Becke, A. D. *Phys. Rev. A* **1988**, *38*, 3098. (a) Becke, A. D. *J. Chem. Phys.* **1993**, *98*, 5648.

(30) Lee, C.; Yang, W.; Parr, R. G. *Phys. Rev. B* **1988**, *37*, 785.

(31) Munzarová, M. L. *Calculation of NMR and EPR Parameters: Theory and Applications*; Kaupp, M., Bühl, M., Malkin, V. G., Eds.; Wiley-VCH Verlag GmgH & Co. KGaA: Weinheim, 2004.

(32) Schaefer, A.; Horn, H.; Ahlrichs, R. *J. Chem. Phys.* **1992**, *97*, 2571. (a) Schaefer, A.; Huber, C.; Ahlrichs, R. *J. Chem. Phys.* **1994**, *100*, 5829.

(33) Reed, A. E.; Weinhold, F. *J. Chem. Phys.* **1983**, *78*, 4066. (a) Peng, C.; Ayala, P. Y.; Schlegel, H. B.; Frisch, M. J. *J. Comput. Chem.* **1996**, *17*, 49.

(34) Godbout, N.; Salahub, D. R.; Andzelm, J.; Wimmer, E. *Can. J. Chem.* **1992**, *70*, 560. (a) Sosa, C.; Andzelm, J.; Elkin, B. C.; Wimmer, E.; Dobbs, K. D.; Dixon, D. A. *J. Phys. Chem.* **1992**, *96*, 6630.

(35) Reuveni, A.; Marcellus, D.; Parker, R. S.; Kwiram, A. L. *J. Chem. Phys.* **1981**, *74*, 179.

(36) Heller, C.; McConnell, H. M. *J. Chem. Phys.* **1960**, *32*, 1535.

(37) Carrington, A.; McLachlan, A. D. *Introduction to Magnetic Resonance*; Harper and Row: New York, 1967.

(38) Box, H. C. *Radiation Effects: ESR and ENDOR Analysis*; Academic Press: New York, 1977.

(39) Wyckoff, R. W. G. *Crystal Structures Vol.5*; John Wiley and Sons: New York, 1966. (a) Kennard, O.; Watson, D. G.; Allen, F. H.; Issacs, N. W., Motherwell, W. D. S.; Pettersen, R. C.; Town, W. G. *Molecular Structures and Dimensions Vol A1: Interatomic Distances 1960−65: Organic and Organometallic Crystal Structures*; Springer: New York, 1972. (b) Harding, M. M. *Acta Crystallogr.* **1999**, *D55*, 1432. (c) Orpen, A. G.; Brammer, L.; Allen, F. H.; Kennard, O.; Watson, D. G.; Taylor, R. *J. Chem. Soc., Dalton Trans.* **1989**, S1–S82. (d) Chakrabarti, P. *Protein Eng.* **1990**, *4*, 57.

(40) Box, H. C.; Freund, H. G.; Lilga, K. T. *J. Chem. Phys.* **1975**, *63*, 2059.

(41) Muto, H.; Iwasaki, M. *J. Chem. Phys.* **1973**, *59*, 4821. (a) Muto, H.; Iwasaki, M.; Takahashi, Y. *J. Chem. Phys.* **1977**, *66*, 1943.

(42) Muto, H.; Iwasaki, M.; Ohkuma, K. *J. Magn. Reson.* **1977**, *25*, 327.

(43) Muto, H.; Nunome, K.; Iwasaki, M. *J. Chem. Phys.* **1974**, *61*, 6311.

(44) Krusic, P. J.; Meakin, P.; Jesson, J. P. *J. Phys. Chem.* **1971**, *75*, 3438.

(45) Larsen, S. C. *J. Phys. Chem. A* **2001**, *105*, 8333.

(46) Saladino, A. C.; Larsen, S. C. *J. Phys. Chem. A* **2002**, *106*, 10444.

(47) McConnell, H. A. *J. Chem. Phys.* **1956**, *24*, 764.

(48) Nelson, W. H.; Gill, C. *Mol. Phys.* **1978**, *36*, 1779.

(49) Pace, M. D.; Christidis, T. C.; Hyde, J. S. *J. Mag. Res. A* **1993**, *102*, 101.

(50) Manikandan, P.; Epel, B.; Goldfarb, D. *Inorg. Chem.* **2001**, *40*, 781.

(51) Smith, II, T. S.; Root, C. A.; Kampf, J. W.; Rasmussen, P. G.; Pecoraro, V. L. *J. Am. Chem. Soc.* **2000**, *122*, 767.

JP811249S